



# Immobilization of phosphonium-based ionic liquid stationary phases extends their operative range to routine applications in the flavor, fragrance and natural product fields



Cecilia Cagliero<sup>a,§,\*</sup>, Humberto Bizzo<sup>b</sup>, Patrizia Rubiolo<sup>a</sup>, Arianna Marengo<sup>a</sup>, Stefano Galli<sup>c</sup>, Jared L. Anderson<sup>d</sup>, Barbara Sgorbini<sup>a</sup>, Carlo Bicchi<sup>a</sup>

<sup>a</sup> Dipartimento di Scienza e Tecnologia del Farmaco, Università degli Studi di Torino, I-10125 Turin, Italy

<sup>b</sup> Embrapa Agroindústria de Alimentos, Avenida das Américas 29501 Rio de Janeiro 23020-470, Brazil

<sup>c</sup> MEGA S.r.l., Via Plinio, 29 - 20025 Legnano MI, Italy

<sup>d</sup> Department of Chemistry, Iowa State University, 50011 Ames Iowa, United States

## ARTICLE INFO

### Article history:

Received 12 October 2021

Revised 29 December 2021

Accepted 30 December 2021

Available online 1 January 2022

### Keywords:

Gas chromatography  
Ionic liquid stationary phases  
Phosphonium-based ionic liquids  
Operative conditions  
Column immobilization  
Flavors  
Fragrances and natural products

## ABSTRACT

Phosphonium-based ionic liquids (ILs) have proven to be successful stationary phases (SPs) for gas chromatography (GC) in several fields of application because of their unique selectivity and good chromatographic properties. This study focuses on the use of two ILs as GC SPs that are based on the phosphonium derivatives trihexyl(tetradecyl)phosphonium chloride ( $[P_{66614}^+][Cl^-]$ ), and trihexyl(tetradecyl)phosphonium bis[(trifluoromethyl)sulfonyl]imide ( $[P_{66614}^+][NTf_2^-]$ ), which have previously been shown to be complementary in terms of chromatographic selectivity and retention. Their application in routine analysis has been limited by their lower maximum allowable operating temperatures (MAOT) (200 °C for the  $[P_{66614}^+][Cl^-]$  IL and 180 °C for  $[P_{66614}^+][NTf_2^-]$ ), which restricts their use to samples that consist of analytes with relatively high volatility. A previous study carried out in the Authors' laboratory focused on extending the use of the  $[P_{66614}^+][Cl^-]$  IL SP to the analysis of samples with analytes of medium-to-low volatility by optimizing column characteristics and operative conditions. This study addresses the immobilization of both the  $[P_{66614}^+][Cl^-]$  and  $[P_{66614}^+][NTf_2^-]$  ILs to the inner wall of fused silica columns to increase their MAOT under soft and hard reaction conditions. The resulting MAOT depended on more or less drastic immobilization conditions, and reached 220 °C for soft immobilization (*So-Im*) and 240 °C for hard immobilization (*Ha-Im*) in the  $[P_{66614}^+][Cl^-]$  IL columns, and 200 °C for *So-Im* and 220° for *Ha-Im* in columns coated with the  $[P_{66614}^+][NTf_2^-]$  IL. The influence of immobilization on the separation power and performance of all the columns has been evaluated using i) the Grob test, ii) a model mixture of 41 compounds of different polarity, structure, and with different organic functional groups representative of the flavor and fragrance field, iii) a standard mixture of 37 fatty acid methyl esters, iv) the peppermint essential oil, v) two mixtures of sesquiterpenic alcohols (farnesols and santalols), and vi) a standard mixture of 16 pesticides. These test samples were also used to demonstrate the complementarity of the two phosphonium-based IL SPs in terms of selectivity and retention.

© 2021 Elsevier B.V. All rights reserved.

## 1. Introduction

Over the past decade, room temperature ionic liquids (ILs) have proven to be successful stationary phases (SPs) for gas chromatography (GC) because of their unique and tunable selectivity, low vapor pressure and volatility, and unique chromatographic properties [1,2]. Their uncommon selectivity, in particular, has made

ILs of great interest for the flavor, fragrance and essential oil (EO) fields and, more generally, for natural product GC analyses as a complement to the most routinely used SPs, which are based on polysiloxane and polyethylene glycol derivatives [3]. Samples in these fields often consist of complex mixtures of isomeric and/or homologous components with similar structural and physical characteristics (e.g. mono- and sesquiterpenoids and phenylpropanoids in EOs) that are challenging to separate in a single run [4–6].

In 2008, Breitbach and Armstrong [7] systematically studied a set of eleven phosphonium-based ILs, characterized them

\* Corresponding author at: Via Pietro Giuria, 9, Torino.

E-mail address: [cecilia.cagliero@unito.it](mailto:cecilia.cagliero@unito.it) (C. Cagliero).

§ <https://orcid.org/0000-0003-3512-6124>

through their physico-chemical properties and their linear solvation energy relationships, and evaluated their use as GC stationary phases. Using inverse GC, they also reported system constants using the Abraham linear solvation energy relationship for the ILs with 34 probe molecules [8]. Their results were the basis for our previous studies on the gas chromatographic properties of two of the derivatives they investigated, namely, trihexyl(tetradecyl)phosphonium chloride,  $[P_{66614}^+][Cl^-]$ , and trihexyl(tetradecyl) phosphonium bis[(trifluoromethyl)sulfonyl]imide,  $[P_{66614}^+][NTf_2^-]$  (Figure S1), and their applicability in the above mentioned fields [9,10].

The choice of these two derivatives was based on their significantly different abilities to interact with solutes through hydrogen bond basicity (the  $a$  coefficient in the Abraham relationship - 6.60 for  $[P_{66614}^+][Cl^-]$  vs. 1.55 for  $[P_{66614}^+][NTf_2^-]$ ) interactions, while the  $e$ ,  $s$ ,  $b$  and  $l$  coefficients are rather similar ( $e$  is indicative of interactions through  $\pi$ - and non-bonding electrons,  $s$  of dipolarity,  $b$  of H-bond acidity and  $l$  of dispersion forces) [8].

These differences result in highly complementary performance when the two ILs are used as GC SPs. A series of experiments carried out with test columns coated with the two phosphonium derivatives demonstrated that the columns coated with the  $[P_{66614}^+][Cl^-]$  IL provided the elution of the analytes in clusters that depend on the compounds chemical class, and a very high retention of oxygenated compounds, while those coated with the  $[P_{66614}^+][NTf_2^-]$  IL showed a general low analyte retention and a more classical elution depending on the polarity and volatility of the compounds [10]. However, the columns coated with both of the investigated ILs showed considerable performance instability in repeated routine analyses, in particular at temperatures above 190–200 °C, where losses of efficiency and poor retention consistency were observed. A further in-depth study was carried out to evaluate the routine stability of the columns coated with the  $[P_{66614}^+][Cl^-]$  IL by submitting them to extensive cycles of stress tests to investigate their operative conditions and limits, consistency of performance over time, and maximum allowable operative temperature (MAOT) [9]. These analyses were first focused on the  $[P_{66614}^+][Cl^-]$  IL SP, although the columns coated with the  $[P_{66614}^+][NTf_2^-]$  IL also behaved in a very similar way. The decrease in efficiency was ascribed to a loss of SP film homogeneity above a critical thickness ( $d_f$ ), which was experimentally determined to be 0.18  $\mu$ m for columns with a 0.25 mm inner diameter ( $d_c$ ), 0.12  $\mu$ m  $d_f$  for columns with 0.18 mm  $d_c$ , and 0.08  $\mu$ m  $d_f$  for columns with 0.10 mm  $d_c$ . The loss of retention has been associated with the possible evaporation of the SP at high temperatures. This explanation was substantiated by research work on the  $[P_{66614}^+][Cl^-]$  IL by Deferm et al., which was published in 2018 and made use of static thermogravimetric analysis (TGA) [11]. The study also discussed a pathway to overcome the limits caused by low MAOT in the analysis of samples containing analytes with medium to low volatility using a suitable combination of i) efficiency and selectivity, and ii) column characteristics and operative conditions. This approach resulted in the elution and successful separation of analytes with medium to low volatility, including FAME analogues within each cluster, up to C24, and diterpenoid alcohols (C20) [9].

Another possible approach for extending the routine use of columns coated with the investigated ILs to include less volatile compounds is to increase the MAOT through their immobilization to the inner wall of the fused silica capillary to avoid evaporation or, at least, to improve their thermal stability. This study aims to develop columns in which the  $[P_{66614}^+][Cl^-]$  and  $[P_{66614}^+][NTf_2^-]$  ILs are immobilized, and to evaluate their performance in terms of stability, MAOT, efficiency and selectivity. The study also focuses on the complementary nature of the performance and selectivity of the two phosphonium-IL-coated columns by analyzing i) the

Grob test, ii) a test mixture of 41 compounds of different polarity and structure with different functional groups that are relevant for the flavor and fragrance field (FFMix), iii) a standard mixture of 37 fatty acid methyl esters (FAMEs), iv) an essential oil, v) two sesquiterpenoid standard mixture containing pairs or groups of compounds that are challenging to separate, and vi) a standard mixture of pesticides.

## 2. Experimental

### 2.1. Samples and chemicals

Trihexyl(tetradecyl)phosphonium chloride,  $[P_{66614}^+][Cl^-]$  (~97%), and trihexyl(tetradecyl)phosphonium bis[(trifluoromethyl)sulfonyl]imide,  $[P_{66614}^+][NTf_2^-]$ , were purchased from Merck (Milan, Italy). The IL was used without further purification.

The following mixtures and samples were used for this study:

- i) the Grob test [12] - peak identification: decane (1), dodecane (2), 1-octanol (3), 2,3-butanediol (4), methyl decanoate (5), methyl undecanoate (E11) (6), methyl dodecanoate (E12) (7), 2,6-dimethylphenol (2,6-DMP) (8), 2,6-dimethylaniline (9), dicyclohexylamine (10), and 2-ethylhexanoic acid (11) in hexane and trichloromethane - was purchased from Merck (Milan, Italy) and analyzed as received;
- ii) a flavor and fragrance standard mixture (FFMix) consisting of 41 compounds. Peak identification:  $\beta$ -pinene (1), limonene (2), nonane (3) (internal standard-ISTD), undecane (4) (ISTD), tridecane (5) (ISTD), 1,8-cineole (6), camphor (7), menthone (8), *i*-menthone (9), pulegone (10), linalyl acetate (11), bornyl acetate (12), menthyl acetate (13), lavandulyl acetate (14), terpinyl acetate (15), ethyl 2-methylbutanoate (16), *trans*- $\beta$ -caryophyllene (17), estragole (18), anethole (19),  $\gamma$ -hexalactone (20),  $\gamma$ -heptalactone (21),  $\gamma$ -octalactone (22), nerol (23), geranial (24), carvone (25), 2-methylbutanol (26), 1-octanol (27), terpinen-4-ol (28), linalool (29),  $\alpha$ -terpineol (30), neomenthol (31), neoi-menthol (32), menthol (33), *i*-menthol (34), lavandulol (35), borneol (36), viridiflorol (37), eugenol (38), *i*-eugenol (39), carvacrol (40), and thymol (41). All compounds were from Merck (Milan, Italy) or from the Authors' standard collection. They were solubilized at a concentration of 100 mg  $L^{-1}$  each in cyclohexane.
- iii) a FAMEs standard solution from Merck (Milan, Italy) consisting of 37 compounds dissolved in methylene chloride. Peak identification: C4:0, C6:0, C8:0, C10:0, C11:0, C12:0, C13:0, C14:0, C14:1c (14), C15:0, C15:1c (15), C16:0, C16:1c (16), C17:0, C17:1c (17), C18:0, C18:1n9c, C18:1n9t, C18:2n6c, C18:2n6t, C18:3n6c, C18:3n3c (18), C20:0, C20:1n9c, C20:2n6c, C20:3n3c, C20:3n6c, C20:4n6c, C20:5n3c (20), C21:0 (21), C22:0, C22:1n9c, C22:2n6c, C22:6n3c (22), C23:0 (23), C24:0, and C24:1n9 (24).
- iv) the essential oil (EO) of peppermint (*Mentha × piperita* L.), which was obtained by hydrodistillation according to the procedure set out in the European Pharmacopoeia [13].
- v) the santalols, farnesols and bergamotol were kindly provided by Dr. D. Joulain, Robertet (Grasse, France). They were solubilized in cyclohexane at a concentration of 1 g  $L^{-1}$  before analysis.
- vi) a pesticide standard mixture, which contained  $\alpha$ -HCH (1), heptachlor (2),  $\beta$ -HCH (3), fonofos (4), chloropyrifos-methyl (5), chloropyrifos-ethyl (6), vinclozolin (7),  $\gamma$ -HCH (8),  $\delta$ -HCH (9), metalaxyl (10), o,p-DDD (11), o,p-DDT (12), hexaconazole (13), p,p'-DDD (14), p,p'-DDT (15), propiconazole (16). They were solubilized at a concentration of 100 mg  $L^{-1}$  each in toluene.

All solvents were HPLC grade from Merck (Milan, Italy).

**Table 1**

Figures of merit of the 6 columns investigated. Legend: *No-Im*: not immobilized, *So-Im*: soft-immobilized, *Ha-Im*: hard-immobilized, MAOT: maximum allowable operative temperature,  $\Delta t$ : retention stability over 20 repeated conditioning cycles (min),  $k$ : retention factor;  $N$ : theoretical plate number,  $N/m$ : theoretical plate number per meter,  $\sigma$ : peak width,  $\Delta s$ : separation number.

Columns	MAOT ( °C)	$\Delta t$ (min) $n = 20$	$k$ 0.4 mL/min	$N$	$N/m$	$\sigma$ (min)	Tailing factor	$\Delta s$ (FFMix)	
$[P_{66614}^+][Cl^-]$		2,6-DMP	<i>Naphthalene</i> ( $T = 80$ °C)						
<i>No-Im</i>	200	0.022	17	69,000	6900	0.027	0.918	1793 (62.0)	
<i>So-Im</i>	220	0.017	12	71,000	7100	0.016	0.956	2108 (55.8)	
<i>Ha-Im</i>	240	0.011	13	73,000	7300	0.020	0.906	2360 (54.6)	
$[P_{66614}^+][NTf_2^-]$		E12	<i>E11</i> ( $T = 90$ °C)						
<i>No-Im</i>	180	0.035	21	62,000	6200	0.023	0.966	1184 (28.2)	
<i>So-Im</i>	200	0.022	12	66,000	6600	0.016	0.914	1351 (25.4)	
<i>Ha-Im</i>	220	0.016	11	65,000	6500	0.017	0.954	1365 (27.3)	

## 2.2. Analysis conditions

### 2.2.1. Instrument set-up

Analyses were carried out on a Shimadzu GC-FID 2010 unit equipped with Shimadzu GC Solution 2.53 U software and a Shimadzu GC 2010 – Shimadzu QP2010-PLUS GC-MS system equipped with GCMS 2.51 software (Shimadzu, Milan, Italy). FID was used to measure chromatographic parameters, and MS for identification purposes.

### 2.2.2. Columns

A list of the  $[P_{66614}^+][Cl^-]$  and  $[P_{66614}^+][NTf_2^-]$  IL columns investigated in this work can be found in Table 1 together with their performance. All columns were from MEGA (Legnano (MI), Italy) and had the same length (10 m), inner diameter,  $d_c$ , (0.1 mm) and film thickness,  $d_f$ , (0.04  $\mu$ m) so as to obtain comparable results. The columns were prepared using the static coating procedure, after a proprietary deactivation process of the fused silica surface. Soft and hard IL-SP immobilization were performed via a proprietary procedure under different operative conditions that MEGA intends to patent. A PEG-based column (MEGA-WAX - 60 m, 0.25 mm  $d_c$   $\times$  0.25  $\mu$ m  $d_f$ ) and a 5%-phenylpolymethylsiloxane – Sil-5%-PH (MEGA-5 - 30 m, 0.25 mm  $d_c$   $\times$  0.25  $\mu$ m  $d_f$ ) from MEGA (Legnano (MI), Italy) were also used for comparison purposes.

### 2.2.3. GC-MS and GC-FID conditions

GC-MS analyses were carried out using the following conditions. Temperatures: injector: 240 °C, transfer line: 240 °C, ion source: 200 °C; carrier gas: He; flow control mode: constant linear velocity, initial flow rate: 0.4 mL/min (linear velocity: 39.7 cm/sec). Each column was connected to the MS through a post-column deactivated of fused silica (0.5 m  $\times$  0.10 mm  $d_c$ ) (MEGA, Legnano, Italy) to make them compatible with an interface temperature that is higher than the MAOT. Injection conditions were: mode: split, split ratio: 1:100; volume: Grob test: 2  $\mu$ L, all other samples 1  $\mu$ L. The same oven temperature program was applied for all experiments with all columns; from 40 °C (1 min) to MAOT (10 min) at 2 °C/min to allow the results to be better compared.

GC-FID analyses were carried out under the following conditions: temperatures: injector: 240 °C, detector: 240 °C; carrier gas: H<sub>2</sub>; initial flow rates: 0.4 mL/min (constant linear velocity: 48.3 cm/sec). All other analysis conditions were the same as those reported in the previous GC-MS paragraph. FID sampling rate: 40 ms. The oven temperature program used was the same as above.

**Analyte identification:** when necessary, analytes were identified using mass spectra and/or linear retention indices. Mass spectra were either compared to those of authentic standards, to those

of commercial or in-house libraries, or literature data. Linear retention indices of the available standards were calculated versus a 100 mg L<sup>-1</sup> C9-C25 hydrocarbon solution, which was prepared in the Authors' laboratory using standards from Merck (Milan, Italy), and analyzed under the above-reported conditions.

### 2.2.4. Column characterization

Each column was characterized using the following parameters (Table 1):

- $[P_{66614}^+][Cl^-]$  IL columns: 1) total theoretical plates (N), number of theoretical plates/meter (N/m) and tailing factor measured isothermally with naphthalene at 80 °C to obtain an average retention factor (k) between 10 and 20 (five repetitions); 2) retention time stability measured using the Grob test on 2,6-DMP (8); 3) the separation measure,  $\Delta s$ , calculated on FFMix between  $\beta$ -pinene (1), the first eluting peak, and eugenol (38), the last eluting peak with all the columns in this group and analyzed under the conditions reported above [14,15].
- $[P_{66614}^+][NTf_2^-]$  IL columns: 1) N, N/m and tailing factor measured isothermally with E11 (6) at 90 °C to obtain k in the same range of the  $[P_{66614}^+][Cl^-]$  columns; 2) retention time stability measured using the Grob test on E12 (7); 3)  $\Delta s$  calculated on FFMix between  $\beta$ -pinene (1), the first eluting peak, and thymol (41), the last eluting peak with all columns of this group and analyzed under the above-reported conditions [14,15].

## 3. Results and discussion

### 3.1. $[P_{66614}^+][Cl^-]$ and $[P_{66614}^+][NTf_2^-]$ ILs as GC stationary phases

The two phosphonium IL SPs have been studied in parallel in this study because their selectivity and retention were expected to vary considerably due to the differences in their hydrogen bond basicity, as indicated by the *a* coefficient in the Abraham relationship. A clear example of this difference can be found in the GC analysis of peppermint essential oil (EO): Fig. 1 reports the analysis of this EO carried out under the same temperature and flow conditions on two narrow bore columns with the same characteristics (l: 10 m,  $d_c$ : 0.10 mm and  $d_f$ : 0.04 mm) coated with the two investigated ILs and compared to the analyses carried out with 5%-phenyl-polymethylsiloxane and polyethyleneglycol 0.25 mm  $d_f$  columns used in routine quality control. The GC patterns with the four columns showed the different selectivity of the four stationary phases, and in particular the analysis with the two investigated IL columns resulted in significantly different analysis times and analyte elution orders. In more detail, the analysis of peppermint EO with the non-immobilized  $[P_{66614}^+][Cl^-]$  IL column took about 43 min for the last eluting peak, lavandulol (27), while

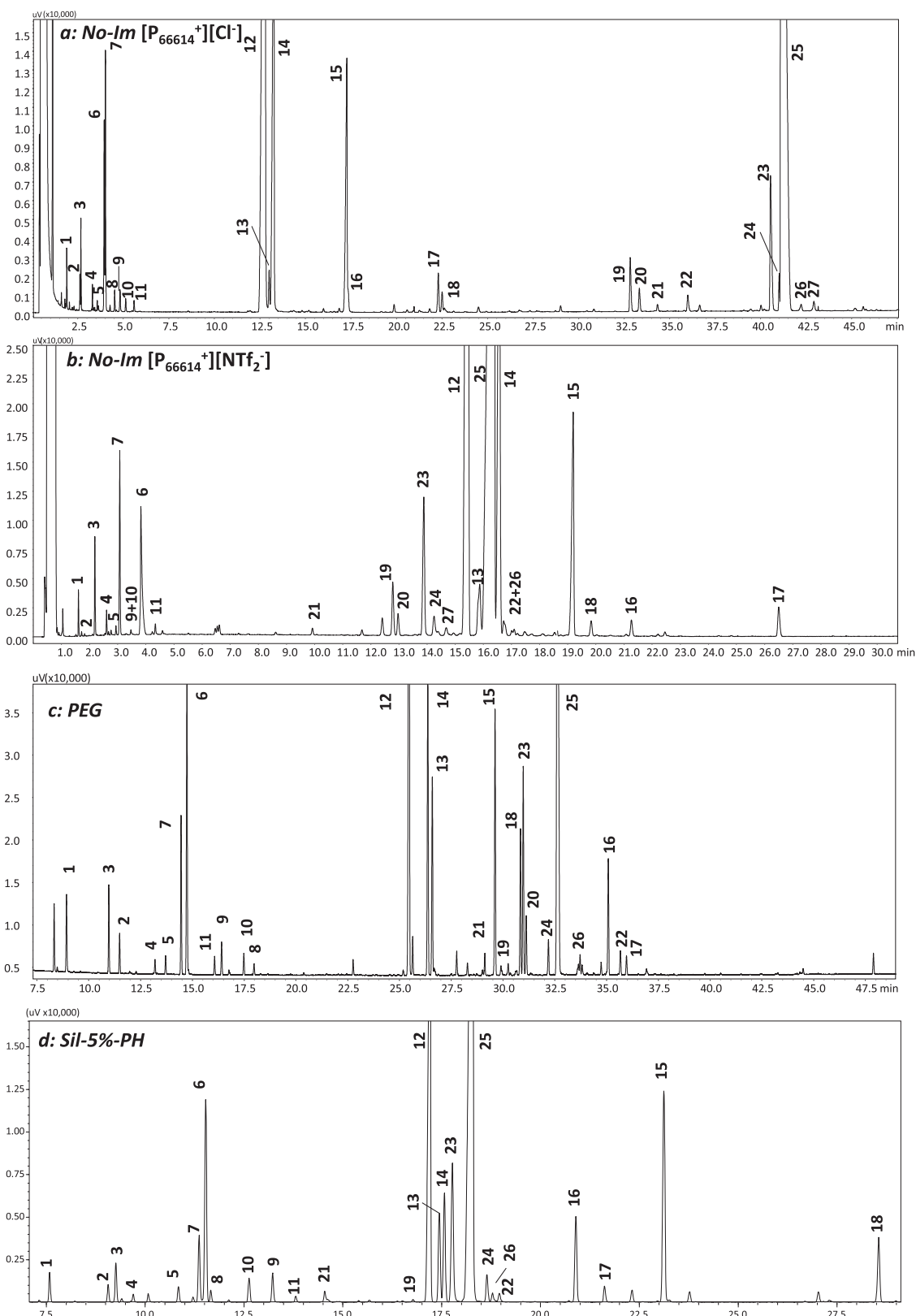


**Fig. 1.** GC-FID patterns of peppermint essential oil analyzed using: a)  $[P_{66614}^+][Cl^-]$  IL column, temp. progr.:  $40\text{ }^\circ\text{C}$  (1 min)/ $2\text{ }^\circ\text{C}/\text{min}/200\text{ }^\circ\text{C}$  (5 min), initial flow rate: 0.4 mL/min; b)  $[P_{66614}^+][NTf_2^-]$  IL column, temp. progr.:  $40\text{ }^\circ\text{C}$  (1 min)/ $15\text{ }^\circ\text{C}/\text{min}/210$  (5 min), initial flow rate: 0.4 mL/min; c) PEG (MEGA-WAX - 60 m, 0.25 mm  $d_c \times 0.25\text{ }\mu\text{m }d_f$ ) column, temp. progr.:  $40\text{ }^\circ\text{C}$  (1 min)/ $3\text{ }^\circ\text{C}/\text{min}/230\text{ }^\circ\text{C}$  (5 min), initial flow rate: 1 mL/min; d) Sil-5%-PH (MEGA-5 - 30 m, 0.25 mm  $d_c \times 0.25\text{ }\mu\text{m }d_f$ ) column, temp. progr.:  $40\text{ }^\circ\text{C}$  (1 min)/ $3\text{ }^\circ\text{C}/\text{min}/250\text{ }^\circ\text{C}$  (5 min), initial flow rate: 1 mL/min. Peak identification: (1)  $\alpha$ -pinene, (2) sabinene, (3)  $\beta$ -pinene, (4)  $\beta$ -myrcene, (5)  $\alpha$ -terpinene, (6) 1,8-cineole, (7) limonene, (8) *cis*-ocimene, (9) *p*-cimene, (10)  $\gamma$ -terpinene, (11)  $\alpha$ -terpinolene, (12) menthone, (13) menthofurane, (14) *i*-menthone, (15) methyl acetate, (16) pulegone, (17) piperitone, (18) *trans*- $\beta$ -caryophyllene, (19) isopulegol, (20) 4-terpineol, (21) linalool, (22)  $\alpha$ -terpineol, (23) neomenthol, (24) neoi-menthol, (25) menthol, (26) *i*-menthol, (27) lavandulol.

the total analysis time was 26 min with the non-immobilized  $[P_{66614}^+][NTf_2^-]$  IL column, with piperitone (**17**) as last eluting peak. Conversely, lavandulol (**27**) elutes after about 15 min with the  $[P_{66614}^+][NTf_2^-]$  IL and piperitone (**17**) after 22 min with the  $[P_{66614}^+][Cl^-]$  IL. Moreover, the main EO component, menthol (**25**), eluted after 41 min with the  $[P_{66614}^+][Cl^-]$  IL and after 16 min with the  $[P_{66614}^+][NTf_2^-]$  IL column. The difference in selectivity is also substantial as the  $[P_{66614}^+][Cl^-]$  IL column exhibits an analyte retention order on the basis of their organic functional groups, i.e., hydrocarbons elute first, then ketones and esters and lastly alcohols, whereas the  $[P_{66614}^+][NTf_2^-]$  IL column separated hydrocarbons from oxygenated compounds well, but within this latter group, the analyte-elution sequence was mainly based on polarity and volatility. This behavior may be linked to the fact that none of the Abraham model coefficients (*e*, *s*, *a*, *b* and *l*) decidedly prevailed over the others, so that specific and/or marked discriminative interactions are generated. These results indicate the presence of significant complementarity between the two phosphonium IL SPs. Their selectivity and chromatographic properties also explain the research work that has been invested in overcoming their MAOT limits and extending their use to the analysis of samples with medium-to-low-volatility analytes: i) by optimizing column characteristics and operative conditions as was reported in a previous article [9]; or ii) by immobilizing them to the fused-silica inner wall of the columns, which is the object of the present study.

### 3.2. Immobilized vs. non-immobilized $[P_{66614}^+][Cl^-]$ and $[P_{66614}^+][NTf_2^-]$ ILs column performance

This section mainly evaluates the performance of two groups of columns; one for each phosphonium IL investigated, with each group in turn consisting of a non-immobilized column (*No-Im*) and two immobilized columns that were submitted to a soft (*So-Im*) and hard (*Ha-Im*) immobilization procedure and to a treatment of the fused silica surface to improve the column inertness (Table 1).

In particular, the performance of the columns was compared internally within each group using several parameters: i) the MAOT and retention stability, measured using 2,6-DMP (**8**) for the  $[P_{66614}^+][Cl^-]$  IL columns and E12 (**7**) for the  $[P_{66614}^+][NTf_2^-]$  IL columns in the Grob test; ii) peak width, tailing factor and efficiency estimated using naphthalene (at 80 °C) for the  $[P_{66614}^+][Cl^-]$  IL columns and E11 (90 °C) for the  $[P_{66614}^+][NTf_2^-]$  IL columns; and iii) the separation measure ( $\Delta s$ ) as calculated using FFMix [9,14]. Table 1 also reports the figures of merits of each column within each group.

The MAOT of each column was measured after a rigorous and standardized conditioning procedure. Each column was conditioned starting from 50 °C and slowly heated up to 180 °C and maintained at that temperature for 12 h. They were then submitted to a series of cycles of 20 runs, each one monitored with the Grob test; each cycle consisted of temperature programs starting from 40 °C to reach a final temperature that was 10 °C higher than the final temperature of the previous cycle (i.e. first cycle: final temperature 190 °C, second cycle: final temperature: 200 °C and so on), with the final isothermal step being held for 10 min. The criterions adopted to evaluate the MAOT were both the stability of the baseline and, more diagnostic, of the analytes retention times. Indeed, by only evaluating column bleeding, Breitbach and Armstrong [7] originally estimated a MAOT of 280 °C for  $[P_{66614}^+][Cl^-]$  and 310 °C for  $[P_{66614}^+][NTf_2^-]$ ; this did not allow them to detect instability in retention times due to stationary phase evaporation at high temperatures [9,11]. The monitoring of the stability of bleeding and retention times resulted in different MAOTs within the set of  $[P_{66614}^+][Cl^-]$  IL columns: 200 °C for the *No-Im* column, 220 °C for the *So-Im* column, and 240 °C for

the *Ha-Im* column. With these MAOTs, the baseline of the three columns was fully stable. The retention of 2,6-DMP (**8**) was highly stable too (Table 1), but was significantly affected by the immobilization process, resulting in a decrease from 57.5 min with the *No-Im* column to approximately 50 min for both the *So-Im* and *Ha-Im* columns. Fig. 2a shows the GC pattern of the Grob test obtained using the three  $[P_{66614}^+][Cl^-]$  columns. The same parameters were measured for the  $[P_{66614}^+][NTf_2^-]$  IL column set, resulting in MAOTs of 180 °C for the *No-Im* column, 200 °C for the *So-Im* column and 220 °C for the *Ha-Im* column. With these MAOTs, the three columns produced a fully stable baseline. In this case too, the retention of E12 (**7**) was highly stable for each column (Table 1), but significantly decreased when using the immobilized columns, dropping from 32 min for the *No-Im* column to nearly 27 min for both the *So-Im* and *Ha-Im* columns. Fig. 2b reports the GC pattern of the Grob test obtained using the three  $[P_{66614}^+][NTf_2^-]$  IL columns.

Peak width efficiency and tailing factor were evaluated with naphthalene at 80 °C for the  $[P_{66614}^+][Cl^-]$  IL columns and with E11 (**6**) at 90 °C for the  $[P_{66614}^+][NTf_2^-]$  IL columns. The adoption of these two compounds and the different analysis temperatures are justified by the need to obtain comparable retention factors within the two groups of columns under the same analysis conditions in order to obtain a more effective comparison of their performance (Table 1) [16]. The results for the  $[P_{66614}^+][Cl^-]$  IL columns, measured with naphthalene, indicated that after full conditioning, the peak width ( $\sigma$ ) slightly decreased with immobilization and that efficiency increased for the immobilized columns. The average theoretical plate number per meter (N/m) over five injections grew from 6900 for the *No-Im* to 7100 for *So-Im* and to 7300 for the *Ha-Im* columns. The peak widths ( $\sigma$ ) improved with immobilization, and ranged from 0.027 min for the *No-Im* column to 0.016 min for the *So-Im* column. The peak widths and efficiencies for the  $[P_{66614}^+][NTf_2^-]$  IL columns, calculated using E11 (**6**), also behaved similarly to the  $[P_{66614}^+][Cl^-]$  IL columns over five replicates and after full conditioning (Table 1). The peak width ( $\sigma$ ) significantly dropped from 0.023 min to about 0.016 min with both immobilization processes. The  $\sigma$  variation contributed to keeping the efficiency (N/m) very similar despite the difference in retention factors, which ranged from 21 for the *No-Im* to 11 for the *Ha-Im* columns. The number of plates per meter varied from 6200 for the *No-Im* column to 6600 for the *So-Im* and 6500 for the *Ha-Im* columns. These results also indicate that immobilization improved SP film stability and homogeneity. Last but not least, the peak tailing of naphthalene measured over 5 replicates using the  $[P_{66614}^+][Cl^-]$  IL columns ranged between 0.906 and 0.956, while that of E11 for the  $[P_{66614}^+][NTf_2^-]$  IL columns varied between 0.966 and 0.914. These results indicate that the inertness of the columns is not affected by the immobilization process. Nevertheless, as expected the peak shapes of some analytes were distorted in various ways, independently on the column technology adopted; this was most evident for dicyclohexylamine (**10**) and 2-ethylhexanoic acid (**11**) on the  $[P_{66614}^+][Cl^-]$  ILs columns, and 2,6-dimethylaniline (**9**) and 2-ethylhexanoic acid (**11**) for the  $[P_{66614}^+][NTf_2^-]$  IL columns. One possible reason may be associated to the surface treatment and immobilization processes that probably produce surface interactions with more polar compounds. This hypothesis may be supported by the full retention of dicyclohexylamine by the immobilised  $[P_{66614}^+][NTf_2^-]$  columns.

The separation performance of the columns was evaluated using the separation measure ( $\Delta s$ ) of each column within each group, calculated using the analysis of the FFMix and determined over the common peaks that covered the widest time range. In particular, the time range between  $\beta$ -pinene (**1**) and eugenol (**38**) was considered for the  $[P_{66614}^+][Cl^-]$  IL columns (*i*-eugenol (**29**), carvacrol (**41**) and thymol (**40**) do not elute with the *No-Im* column

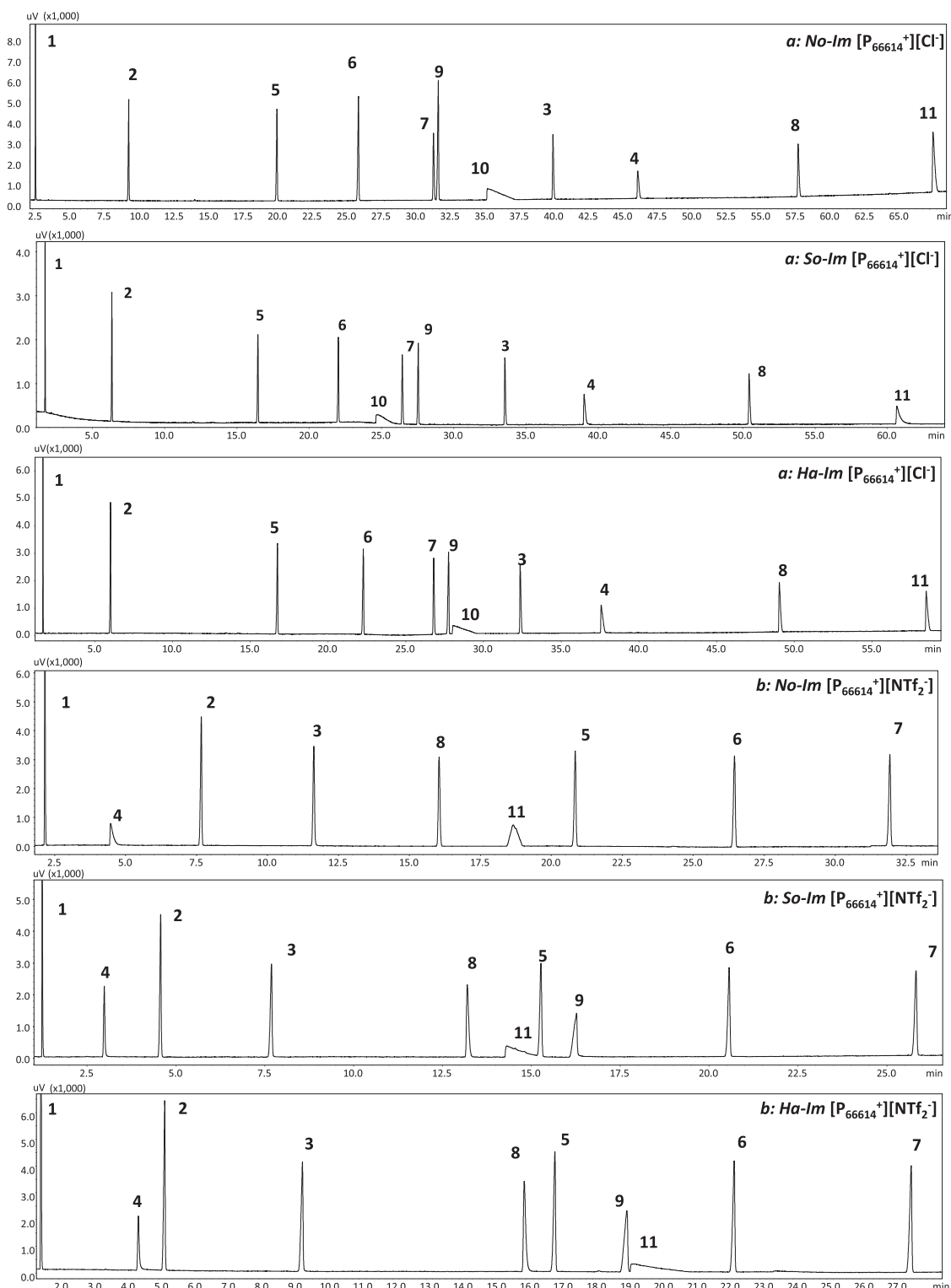


**Fig. 2.** GC-FID patterns of the Grob test analyzed after full conditioning with: (a) *No-Im*, *So-Im* and *Ha-Im*  $[P_{66614}^+][Cl^-]$  IL columns; (b) *No-Im*, *So-Im* and *Ha-Im*  $[P_{66614}^+][NTf_2^-]$  IL columns. Temperature program: 40 °C (1 min)/2 °C/min/MAOT(5 min), initial flow rate: 0.4 mL/min. . Peak identification: decane (1), dodecane (2), 1-octanol (3), 2,3-butanediol (4), methyl decanoate (5), methyl undecanoate (E11) (6), methyl dodecanoate (E12) (7), 2,6-dimethylphenol (2,6-DMP) (8), 2,6-dimethylaniline (9), dicyclohexylamine (10), and 2-ethylhexanoic acid (11).

because of its low MAOT) and the time range between  $\beta$ -pinene (**1**) and thymol (**41**) was used for the  $[P_{66614}^+][NTf_2^-]$  IL. The results show that the immobilization for both groups of columns positively influenced  $\Delta s$  (Table 1), which ranged between 1793 for the *No-Im* and 2360 for the *Ha-Im*  $[P_{66614}^+][Cl^-]$  IL columns, with an increase of about 24%, and between 1184 for the *No-Im* and 1365 for the *Ha-Im*  $[P_{66614}^+][NTf_2^-]$  IL columns, with an improvement of about 13%. In this case again, within each group of columns, the *So-Im* performed in between the *Ha-Im* and the *No-Im* columns and closer to the *Ha-Im*; the  $\Delta s$  was 2108 for the *So-Im*-  $[P_{66614}^+][Cl^-]$  and 1351 for the *So-Im*- $[P_{66614}^+][NTf_2^-]$  ILs.

The effects of the immobilization process on column selectivity were evaluated within each group of columns, while a detailed examination of the complementarity of the  $[P_{66614}^+][Cl^-]$  and  $[P_{66614}^+][NTf_2^-]$  IL stationary phases will be the objective of a dedicated paragraph below. Attention was first focused on two standard mixtures that are characterized by components with different structures, polarity and organic functions, (i.e., the Grob test with eleven components and FFMix with forty-one compounds). The results of the Grob test show that immobilization does not influence the selectivity of the columns within each group. Moreover, the  $[P_{66614}^+][Cl^-]$  IL columns maintain the following elution order: hydrocarbons, esters, nitrogen derivatives, hydroxyl derivatives and carboxylic acids, and confirm the aforementioned decrease in retention with the immobilized column. The improvement in the peak shape with increase in strength of immobilization, compared to the *No-Im* column, is of particular relevance and is clearly shown by 2,6-dimethylaniline (**9**), and to a lesser extent by 2-ethylhexanoic acid (**11**) (Fig. 2a and 2b). The only exception is dicyclohexylamine (**10**), whose elution is conditioned by an intrinsic characteristic of the stationary phase (hydrogen bond basicity) and results in a distorted peak with unstable retention compared to the other components. The results are confirmed in the  $[P_{66614}^+][NTf_2^-]$  IL columns that show similar selectivity, a decrease in retention with immobilization, and an order of elution that is significantly conditioned by analyte volatility. With the *No-Im* column, both nitrogen derivatives were fully retained and the 2,3-butanediol (**4**) and 2-ethylhexanoic acid (**11**) peaks were rather distorted. In addition, the latter also presents unstable retention relative to the other components. Conversely, immobilization enabled the elution of 2,6-dimethylaniline (**9**), but not dicyclohexylamine (**10**). The *So-Im* column provided better chromatographic performance than *Ha-Im*, with a general improvement in the peak shapes, particularly for 2,3-butanediol (**4**) and hydroxyl derivatives.

The results obtained with FFMix using the two column groups were consistent with those obtained with the Grob test. Immobilized  $[P_{66614}^+][Cl^-]$  IL stationary phases again separated according to organic function (Fig. 3a). In addition, both immobilized columns enabled the elution of *i*-eugenol (**39**), thymol (**40**) and carvacrol (**41**), thanks to their higher MAOT, that were not eluted with the *No-Im* column. Again, carbonyl-derivative analytes eluted in the order ketones, esters, aldehydes and lactones. Similar considerations can be made for hydroxyl derivatives as the immobilization of the stationary phase does not influence their elution order, i.e. acyclic and cyclic alcohols followed by aromatic derivatives (phenols). The *So-Im*  $[P_{66614}^+][Cl^-]$  IL column baseline separated all forty-one FFMix components.

Immobilized  $[P_{66614}^+][NTf_2^-]$  IL columns also maintained the separation properties of the *No-Im* column as they were able to discriminate hydrocarbons and highly volatile apolar compounds from oxygenated compounds with an elution order that is primarily driven by volatility and polarity (Fig. 3b). Also, in this case both immobilized columns enabled the elution of viridiflorol (**37**), which did not elute with the *No-Im* column, probably due to irreversible adsorption. Some variations in the order of analyte elution were observed in the *No-Im* and immobilized columns, but they were

all within a limited range of elution temperatures, which confirms the importance of volatility in the selectivity of this phosphonium-based IL-SP. Both immobilized columns provided coherent patterns with the *No-Im* column and better separation, with the *So-Im* column providing the best results in terms of baseline separation and peak shape.

Different results were obtained for the FAME standard mixture, which included 37 components with of carbon atom numbers (CN) between C4 and C24. The immobilization of  $[P_{66614}^+][Cl^-]$  and  $[P_{66614}^+][NTf_2^-]$  IL SPs notably affected their separation in some cases. Both groups of columns provided very good FAME separation according to their CN, with the main differences being observed within clusters of the same CN. Fig. 4 reports the chromatographic patterns from CN 14 to CN 24, obtained on the six investigated columns. The  $[P_{66614}^+][Cl^-]$  IL group of columns showed the most remarkable variations. The *No-Im* column only eluted FAME homologues up to C20 because of its limited MAOT (200 °C), while both immobilized columns eluted all of the homologues up to C24. The *No-Im* and *So-Im* columns separated both components of the C14 and C15 pairs, while they co-eluted with the *Ha-Im*-column. Special attention was paid to three clusters C18, C20 and C22; C18 and C20 consist of seven compounds, and C22 is made up of four. The *No-Im* and *So-Im* columns separated six compounds out of seven for each of the two clusters, while *Ha-Im* separated all C20 components and six out of seven for C18. On the other hand, the *So-Im* column was the only column that was able to separate the four components of the C22 cluster. It is worth noting that the saturated FAMEs within each CN always eluted as the last peak of the cluster with the *No-Im* column, while the saturated C18 and C20 "moved" inside the clusters when using the immobilized columns, with this effect increasing from *So-Im* to *Ha-Im*. Differences were also observed with the  $[P_{66614}^+][NTf_2^-]$  set of columns. The *No-Im*  $[P_{66614}^+][NTf_2^-]$  IL column separated the homologues up to the C22:6 FAMEs despite its low MAOT (180 °C), and both immobilized columns eluted all components up to C24. All of the columns in this group separated both components of the C14 and C17 pairs, and maintained the elution order for all components. The three complex clusters, C18, C20, and C22, behaved coherently across the three columns. The best result with cluster C18 was obtained using the *Ha-Im* column, which separated six out of seven components compared to five with *So-Im* and four with the *No-Im*. Six out of seven components of the C20 cluster were baseline separated by all three columns. As with the  $[P_{66614}^+][Cl^-]$  IL, the *Ha-Im* column separated all four components of the C22 cluster (although not achieving baseline resolution), while the *No-Im* and *So-Im* columns separated three out of four components. Interestingly, unlike the  $[P_{66614}^+][Cl^-]$  IL columns, immobilized  $[P_{66614}^+][NTf_2^-]$  IL columns maintained both the elution order within each CN cluster, and the saturated FAMEs as the last peaks. A comparison of the results obtained on the same standard sample using the *Ha-Im*  $[P_{66614}^+][NTf_2^-]$  IL column with the existing conventional and IL-based SPs, the latter ever more frequently being used for FAME analyses [17–19], showed a more clear net separation of the clusters as a function of their CN, with the saturated FAMEs in the last position. However, as mentioned above, there was one co-elution in both the C18 and C20 group of peaks.

### 3.3. Complementarity of $[P_{66614}^+][Cl^-]$ and $[P_{66614}^+][NTf_2^-]$ ILs as GC stationary phases

The GC selectivities and retention properties of the two phosphonium-based SPs investigated herein differ drastically, but are highly complementary. These differences are easily perceivable both in terms of retention, which is generally rather high for the same analyte with the  $[P_{66614}^+][Cl^-]$  IL SP and drastically lower with  $[P_{66614}^+][NTf_2^-]$  IL under the same analytical conditions, and

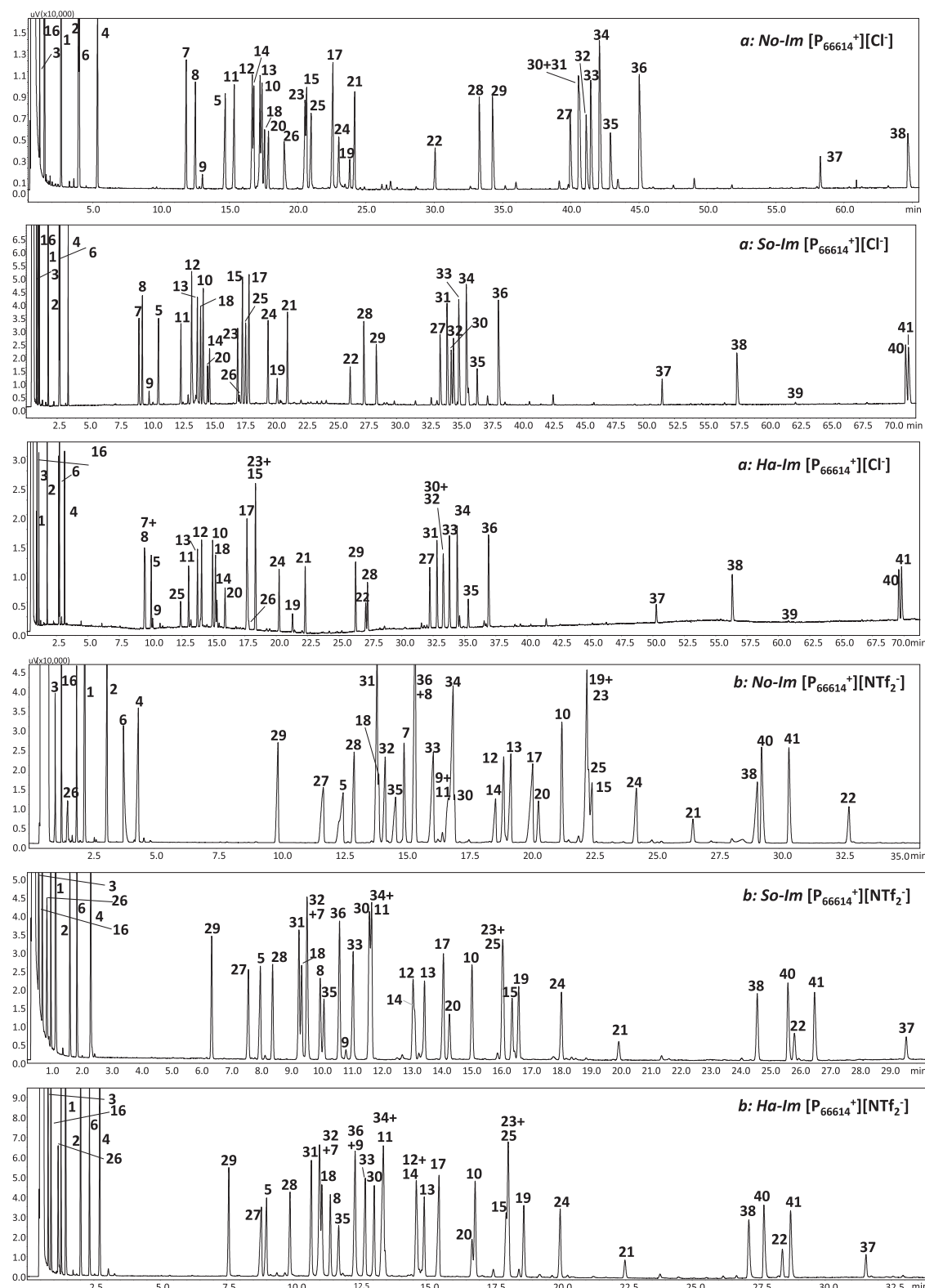


**Fig. 3.** GC-FID patterns of FFMIX analyzed with: (a) *No-Im*, *So-Im* and *Ha-Im*  $[P_{66614}^+][Cl^-]$  columns; (b) *No-Im*, *So-Im* and *Ha-Im*  $[P_{66614}^+][NTf_2^-]$  IL columns. Temperature program: 40 °C (1 min)/2 °C/min/MAOT(5 min), initial flow rate: 0.4 mL/min. Peak identification:  $\beta$ -pinene (1), limonene (2), nonane (3) (ISTD), undecane (4) (ISTD), tridecane (5) (ISTD), 1,8-cineole (6), camphor (7), menthone (8), *i*-menthone (9), pulegone (10), linalyl acetate (11), bornyl acetate (12), menthyl acetate (13), lavandulyl acetate (14), terpinyl acetate (15), ethyl 2-methylbutanoate (16), *trans*- $\beta$ -caryophyllene (17), estragole (18), anethole (19),  $\gamma$ -hexalactone (20),  $\gamma$ -heptalactone (21),  $\gamma$ -octalactone (22), nerol (23), geranial (24), carvone (25), 2-methylbutanol (26), 1-octanol (27), terpinen-4-ol (28), linalool (29),  $\alpha$ -terpineol (30), neomenthol (31), neoi-menthol (32), menthol (33), *i*-menthol (34), lavandulol (35), borneol (36), viridiflorol (37), eugenol (38), *i*-eugenol (39), carvacrol (40), and thymol (41).

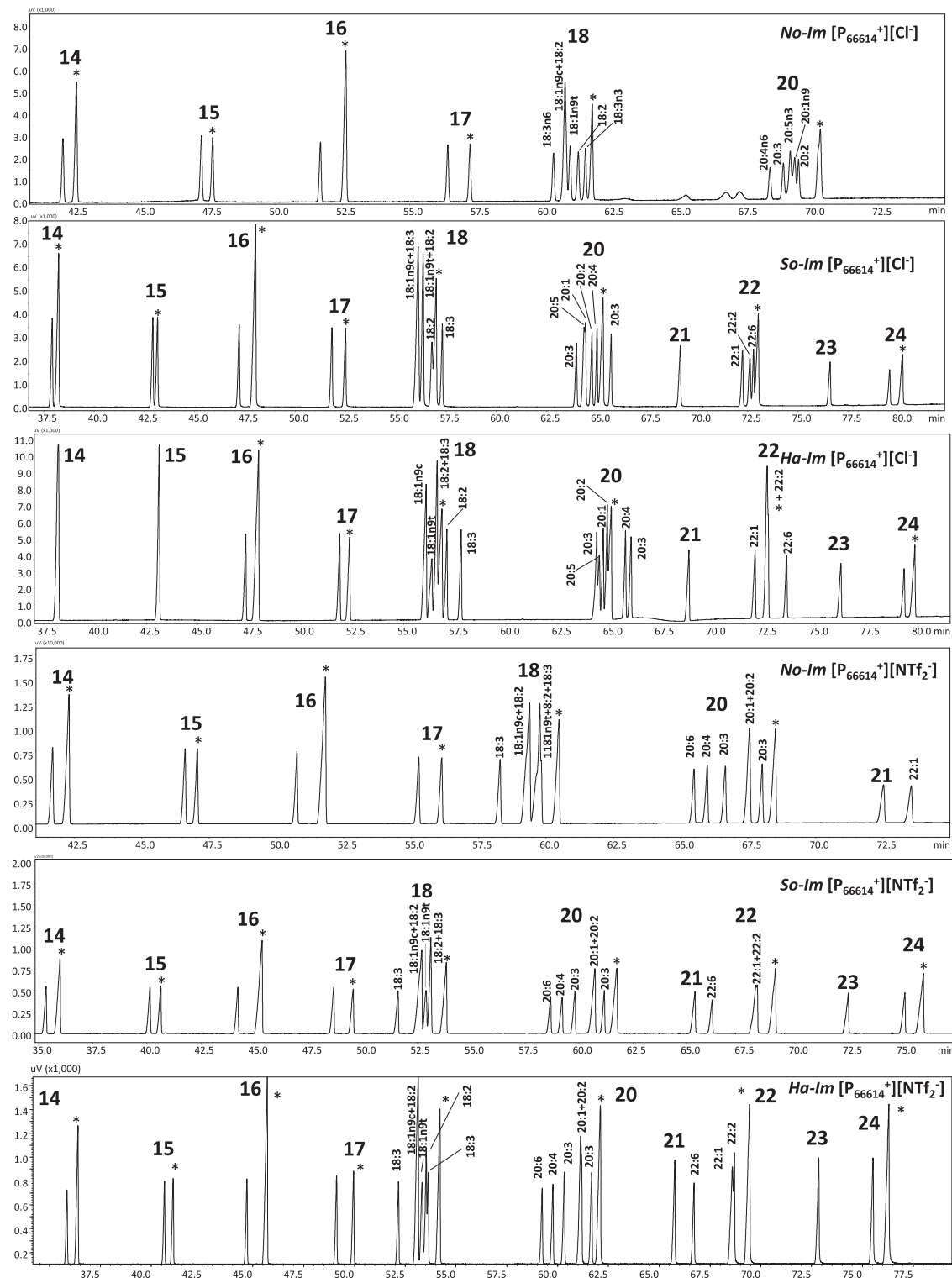


**Fig. 4.** GC-FID patterns of the FAME standard mixture analyzed from C14 to C24 with: (a) No-Im, So-Im and Ha-Im  $[P_{66614}^+][Cl^-]$  columns; (b) No-Im, So-Im and Ha-Im  $[P_{66614}^+][NTf_2^-]$  IL columns. Temperature program: 40 °C (1 min)/2 °C/min/MAOT(5 min), initial flow rate: 0.4 mL/min. Peak identification: C4:0, C6:0, C8:0, C10:0, C11:0, C12:0, C13:0, C14:0, C14:1c (**14**), C15:0, C15:1c (**15**), C16:0, C16:1c (**16**), C17:0, C17:1c (**17**), C18:0, C18:1n9c, C18:1n9t, C18:2n6c, C18:3n6c, C18:3n3c (**18**), C20:0, C20:1n9c, C20:2n6c, C20:3n6c, C20:3n6c, C20:4n6c, C20:5n3c (**20**), C21:0 (**21**), C22:0, C22:1n9c, C22:2n6c, C22:6n3c (**22**), C23:0 (**23**), C24:0, and C24:1n9 (\*): saturated FAME.

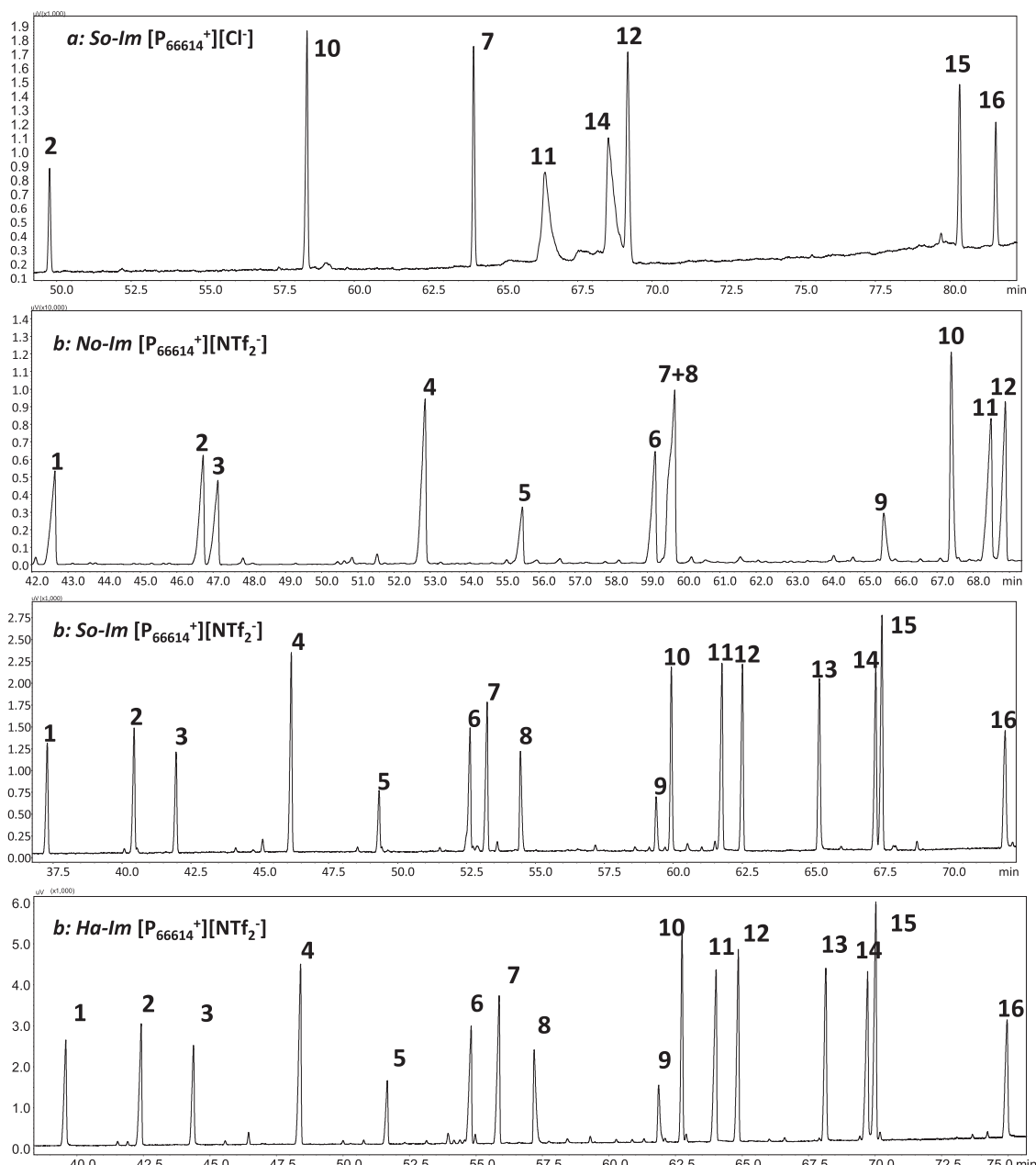


**Fig. 5.** GC-FID patterns of pesticide standard mixture analyzed with: (a) *So-Im*  $[P_{66614}^+][Cl^-]$  IL column; (b) *No-Im*, *So-Im* and *Ha-Im*  $[P_{66614}^+][NTf_2^-]$  IL columns. Temperature program: 40 °C (1 min)/2 °C/min/MAOT(5 min), initial flow rate: 0.4 mL/min. Peak identification: -HCH (1), heptachlor (2),  $\beta$ -HCH (3), fonofos (4), chloropyrifos-methyl (5), chloropyrifos-ethyl (6), vinclozolin (7),  $\gamma$ -HCH (8),  $\delta$ -HCH (9), metalaxyl (10), o,p-DDD (11), o,p-DDT (12), hexaconazole (13), p,p'-DDD (14), p,p'-DDT (15), propiconazole (16).

selectivity, which can be explained with the high hydrogen bond basicity of  $[P_{66614}^+][Cl^-]$  IL ( $\alpha$  coefficient in the Abraham relationship). The lower retention of  $[P_{66614}^+][NTf_2^-]$  IL columns also results in lower elution temperatures for medium-to-low-volatility analytes, which partially overcomes its limited MAOT (max 220 °C for the *Ha-Im* column). Therefore, this feature makes it possible to perform the GC analysis of samples that cannot be analyzed with the  $[P_{66614}^+][Cl^-]$  IL columns, as is the case with the standard mixture of pesticides, as reported in Fig. 5.

None of the investigated  $[P_{66614}^+][Cl^-]$  IL columns eluted all of the pesticides in the analyzed standard mixture, and this is probably because the highest temperatures achieved were not sufficient. The best results were obtained with the *So-Im* column, from which eight pesticides out of sixteen eluted (Fig. 5a). The situation with the  $[P_{66614}^+][NTf_2^-]$  IL SP from which, under the applied condi-

tions, not all pesticides eluted with the *No-Im* column (12 on 16) is different. However, they all eluted and were well separated when using both immobilized columns (Figs. 5b). Column immobilization did not affect the elution order with either of the investigated IL SPs.

Conversely, the  $[P_{66614}^+][Cl^-]$  IL columns successfully separated the standard mixture of farnesols, bergamotol and santalols, which are characteristic components of sandalwood EO (*Santalum* spp.), well known for its importance in the perfume industry [20]. This IL SP successfully separates the acyclic sesquiterpene alcohols (farnesols,  $C_{15}H_{26}O$ , MW: 222) from the cyclic sesquiterpene alcohols (santalols and bergamotol,  $C_{15}H_{24}O$ , MW: 220), as well as each isomer within its own group (Fig. 6a). On the other hand, the  $[P_{66614}^+][NTf_2^-]$  IL columns did not discriminate between the cyclic and acyclic sesquiterpene alcohols, with some of them ((E)-

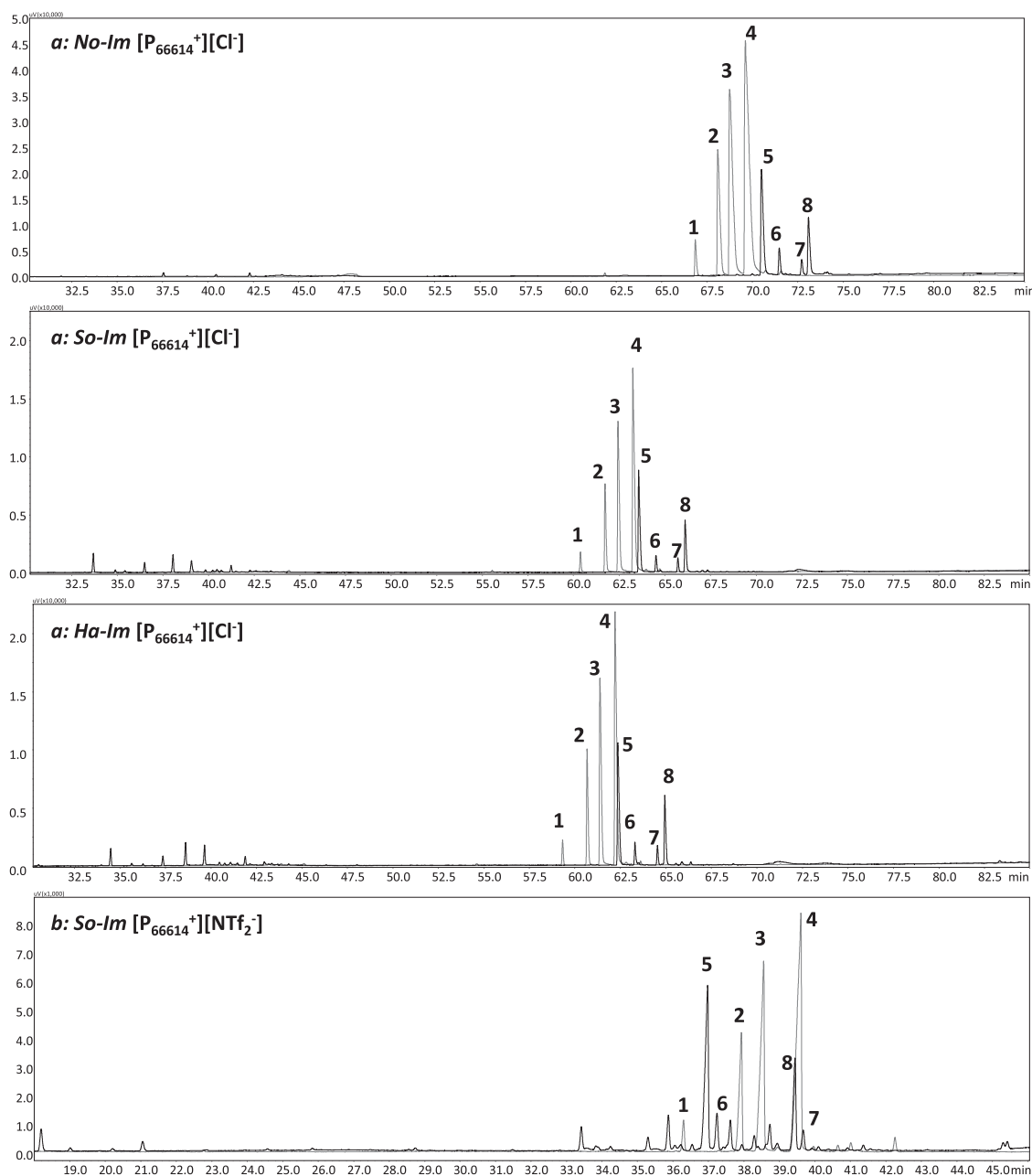


**Fig. 6.** GC-FID patterns of santalol (black profiles) and farnesol (pink profiles) standard mixture analyzed with: (a) *No-Im*, *So-Im* and *Ha-Im*  $[P_{66614}^+][Cl^-]$  IL columns; (b) *So-Im*  $[P_{66614}^+][NTf_2^-]$  IL column. Temperature program: 40 °C (1 min)/2 °C/min/MAOT(5 min), initial flow rate: 0.4 mL/min. Peak identification: (Z,E)-farnesol (1), (E,Z)-farnesol (2), (Z,E)-farnesol (3), (E,E)-farnesol (4), (Z)-α-santalol (5), (Z)-α-bergamotol (6), epi-β-santalol (7), (Z)-β-santalol (8).

farnesol (4), (Z)-β-santalol, (8) and epi-β-santalol (7)) co-eluting (Fig. 6b). This behavior is probably due to the lack of a suitable predominant characteristic in the Abraham linear solvation energy relationship for this IL SP, which does not allow structure-specific selective interactions to occur other than those based on volatility and polarity. In this example, immobilization affects column retention differently; the order of analyte elution of all the  $[P_{66614}^+][Cl^-]$  IL columns was the same, while it changed within the sesquiterpene alcohol clusters for  $[P_{66614}^+][NTf_2^-]$  IL, from *No-Im* to *Ha-Im*.

#### 4. Conclusion

The reported results show that the two investigated phosphonium-based ILs can successfully be used as SPs for

gas chromatography because of their complementarity as well as uncommon selectivity. Their immobilization contributed to overcoming the low MAOT of the columns coated with non-immobilized IL-based SPs. IL immobilization grants higher thermal stability and consistency of performance, with slight changes in the selectivity for a very limited number of compounds. Column MAOT depends on the conditions of the immobilization process, with 220 °C being reached for the *So-Im* and 240 °C for the *Ha-Im*  $[P_{66614}^+][Cl^-]$  IL columns, and 200 °C being reached for the *So-Im* and 220 °C for the *Ha-Im* columns coated with  $[P_{66614}^+][NTf_2^-]$  IL. The increased MAOT allowed the complementarity of the chromatographic properties of the two SPs to be better exploited, enabled the analysis of compounds with rather low volatility, such as pesticides, and allowed groups of analogous compounds with similar molecular weights and organic functions to be discrimi-

nated on the basis of one of their structural characteristics (e.g. acyclic and cyclic sesquiterpene alcohols).

This aspect of the study was based on columns with the same characteristics, and analyses carried out under the same conditions in order to better compare SP performance based on selectivity and retention. Further studies to optimize separation and analysis time by modifying column characteristics (length, inner diameter and film thickness) and operative conditions (temperature program and flow rate) are underway on real world samples to make these SPs suitable for routine analyses.

### Declaration of Competing Interest

The authors declare that they have no known competing financial interests or personal relationships that could have appeared to influence the work reported in this paper.

The authors declare the following financial interests/personal relationships which may be considered as potential competing interests.

### CRediT authorship contribution statement

**Cecilia Cagliero:** Investigation, Conceptualization, Methodology, Writing – review & editing. **Humberto Bizzo:** Investigation, Data curation, Writing – review & editing. **Patrizia Rubiolo:** Data curation, Writing – review & editing. **Arianna Marengo:** Data curation, Writing – review & editing. **Stefano Galli:** Resources, Conceptualization, Writing – review & editing. **Jared L. Anderson:** Resources, Conceptualization, Writing – review & editing. **Barbara Sgorbini:** Data curation, Writing – review & editing. **Carlo Bicchi:** Conceptualization, Methodology, Supervision, Writing – original draft.

### Acknowledgements

This research project was financially supported by the 'Ricerca Locale' (Ex60%2019) project of the University of Turin, Turin (Italy). J.L.A. acknowledges funding from the Chemical Measurement and Imaging Program at the National Science Foundation (Grant No. CHE-1709372).

### Supplementary materials

Supplementary material associated with this article can be found, in the online version, at doi:[10.1016/j.chroma.2021.462796](https://doi.org/10.1016/j.chroma.2021.462796).

### References

- [1] D.W. Armstrong, L. He, Y.S. Liu, Examination of ionic liquids and their interaction with molecules, when used as stationary phases in gas chromatography, *Anal. Chem.* 71 (17) (1999) 3873–3876, doi:[10.1021/ac990443p](https://doi.org/10.1021/ac990443p).
- [2] M.J. Trujillo-Rodríguez, H. Nan, M. Varona, M.N. Emaus, I.D. Souza, J.L. Anderson, Advances of ionic liquids in analytical chemistry, *Anal. Chem.* 91 (1) (2019) 505–531, doi:[10.1021/acs.analchem.8b04710](https://doi.org/10.1021/acs.analchem.8b04710).
- [3] C. Cagliero, C. Bicchi, Ionic liquids as gas chromatographic stationary phases: how can they change food and natural product analyses? *Anal. Bioanal. Chem.* 412 (1) (2020) 17–25, doi:[10.1007/s00216-019-02288-x](https://doi.org/10.1007/s00216-019-02288-x).
- [4] C. Cagliero, B. Sgorbini, C. Cordero, E. Liberto, C. Bicchi, P. Rubiolo, Analytical strategies for multipurpose studies of a plant volatile fraction, in: K. Hostettmann, H. Stuppner, A. Marston, S. Chen (Eds.), *Encyclopedia of Analytical Chemistry*, John Wiley & Sons, Ltd, 2014, pp. 447–466, doi:[10.1002/9780470027318.a9919](https://doi.org/10.1002/9780470027318.a9919).
- [5] P. Rubiolo, C. Cagliero, C. Cordero, E. Liberto, B. Sgorbini, C. Bicchi, Gas chromatography in the analysis of flavours and fragrances, in: K. Dettmer-Wilde, W. Engewald (Eds.), *Practical Gas Chromatography: A Comprehensive Reference*, Springer Berlin Heidelberg, Berlin, Heidelberg, 2014, pp. 717–743, doi:[10.1007/978-3-642-54640-2\\_20](https://doi.org/10.1007/978-3-642-54640-2_20).
- [6] P. Rubiolo, E. Liberto, B. Sgorbini, R. Russo, J.L. Veuthey, C. Bicchi, Fast-GC – Conventional quadrupole mass spectrometry in essential oil analysis, *J. Sep. Sci.* 31 (6–7) (2008) 1074–1084, doi:[10.1002/jssc.200700577](https://doi.org/10.1002/jssc.200700577).
- [7] Z.S. Breitbach, D.W. Armstrong, Characterization of phosphonium ionic liquids through a linear solvation energy relationship and their use as GLC stationary phases, *Anal. Bioanal. Chem.* 390 (6) (2008) 1605–1617, doi:[10.1007/s00216-008-1877-3](https://doi.org/10.1007/s00216-008-1877-3).
- [8] M.H. Abraham, C.F. Poole, S.K. Poole, Classification of stationary phases and other materials by gas chromatography, *J. Chromatogr. A* 842 (1) (1999) 79–114 [https://doi.org/https://doi.org/10.1016/S0021-9673\(98\)00930-3](https://doi.org/https://doi.org/10.1016/S0021-9673(98)00930-3).
- [9] C. Cagliero, M. Mazzucotelli, P. Rubiolo, A. Marengo, S. Galli, J.L. Anderson, B. Sgorbini, C. Bicchi, Can the selectivity of phosphonium based ionic liquids be exploited as stationary phase for routine gas chromatography? A case study: the use of trihexyl(tetradecyl) phosphonium chloride in the flavor, fragrance and natural product fields, *J. Chromatogr. A* 1619 (2020) 460969 <https://doi.org/https://doi.org/10.1016/j.chroma.2020.460969>.
- [10] M. Mazzucotelli, C. Bicchi, A. Marengo, P. Rubiolo, S. Galli, J.L. Anderson, B. Sgorbini, C. Cagliero, Ionic liquids as stationary phases for gas chromatography–Unusual selectivity of ionic liquids with a phosphonium cation and different anions in the flavor, fragrance and essential oil analyses, *J. Chromatogr. A* 1583 (2019) 124–135, doi:[10.1016/j.chroma.2018.11.032](https://doi.org/10.1016/j.chroma.2018.11.032).
- [11] C. Deferm, A. Van Den Bossche, J. Luyten, H. Oosterhof, J. Fransaer, K. Binnemans, Thermal stability of trihexyl(tetradecyl)phosphonium chloride, *Phys. Chem. Chem. Phys.* 20 (4) (2018) 2444–2456, doi:[10.1039/c7cp08556g](https://doi.org/10.1039/c7cp08556g).
- [12] K. Grob, G. Grob, K. Grob Jr, Testing capillary gas chromatographic columns, *J. Chromatogr. A* 219 (1) (1981) 13–20, doi:[10.1016/S0021-9673\(00\)80568-3](https://doi.org/10.1016/S0021-9673(00)80568-3).
- [13] European Pharmacopoeia, 10th Edn., 2021.
- [14] L.M. Blumberg, Metrics of separation performance in chromatography. Part 1. Definitions and application to static analyses, *J. Chromatogr. A* 1218 (32) (2011) 5375–5385, doi:[10.1016/j.chroma.2011.06.017](https://doi.org/10.1016/j.chroma.2011.06.017).
- [15] L.M. Blumberg, Metrics of separation performance in chromatography: part 2. Separation performance of a heating ramp in temperature-programmed gas chromatography, *J. Chromatogr. A* 1244 (2012) 148–160, doi:[10.1016/j.chroma.2012.04.053](https://doi.org/10.1016/j.chroma.2012.04.053).
- [16] C.F. Poole, N. Lenca, Gas chromatography on wall-coated open-tubular columns with ionic liquid stationary phases, *J. Chromatogr. A* 1357 (2014) 87–109 <https://doi.org/https://doi.org/10.1016/j.chroma.2014.03.029>.
- [17] K. Dettmer, Assessment of ionic liquid stationary phases for the GC analysis of fatty acid methyl esters, *Anal. Bioanal. Chem.* 406 (20) (2014) 4931–4939, doi:[10.1007/s00216-014-7919-0](https://doi.org/10.1007/s00216-014-7919-0).
- [18] C. Fanali, G. Micalizzi, P. Dugo, L. Mondello, Ionic liquids as stationary phases for fatty acid analysis by gas chromatography, *Analyst* 142 (24) (2017) 4601–4612, doi:[10.1039/c7an01338h](https://doi.org/10.1039/c7an01338h).
- [19] A. Vickers, High-efficiency FAME analysis using capillary GC, *Am. Lab.* 39 (2007) 18–20.
- [20] N. Baldovini, C. Delasalle, D. Joulain, Phytochemistry of the heartwood from fragrant *Santalum* species: a review, *Flavour Frag. J.* 26 (1) (2011) 7–26, doi:[10.1002/ffj.2025](https://doi.org/10.1002/ffj.2025).